https://doi.org/10.1016/j.engstruct.2021.111897

1 **Title: Extended CSDT model for shear capacity assessments of bridge deck slabs** 2

Running head: Shear capacity of bridge deck slabs with the CSDT model

8

Author 1
P.h.D. candidate Alex M. D. de Sousa
University of São Paulo, São Carlos School of Engineering
Department of Structural Engineering
Av. Trabalhador Sãocarlense, 400, 13566-590,
Sao Carlos, Brazil
Phone: (+55) 16 3373 9474
Orcid ID: 0000-0003-0424-4080
alex_dantas@usp.br

Author 2
Dr. ir. Eva O.L. Lantsoght
Politécnico, Universidad San Francisco de Quito
Diego de Robles y Pampite, Cumbaya, Quito, Ecuador
Phone: (+593) 2 297-1700
Orcid ID: 0000-0003-4548-7644
elantsoght@usfq.edu.ec
Concrete Structures, Delft University of Technology
P.O. Box 5048, 2600 GA Delft, The Netherlands
E.O.L.Lantsoght@tudelft.nl

Author 3
Dr. ir. Yuguang Yang
Concrete Structures, Delft University of Technology,
P.O. Box 5048, 2600 GA Delft, The Netherlands
yuguang.yang@tudelft.nl

Author 4
Dr. ir. Mounir K. El Debs
University of São Paulo, São Carlos School of Engineering,
Department of Structural Engineering,
Av. Trabalhador Sãocarlense, 400, 13566-590,
São Carlos, Brazil
Phone: (+55) 16 3373 9474
Orcid ID: 0000-0001-5955-7936
mkdebs@sc.usp.br

9

10 **Abstract**

11

12 The shear strength evaluation of reinforced concrete bridge deck slabs by accurate models can 13 indicate strength reserves and avoid costly operations necessary for the extension of their lifetime. 14 This article introduces an approach that extends the Critical Shear Displacement Theory model 15 (CSDT) for reaching higher levels of approximation of the shear strength for slabs subjected to 16 concentrated loads close to the support. A database with 141 tests of wide reinforced concrete 17 members under concentrated loads close to the support failing in one-way shear was built. The tests 18 represented typical loads in bridge slabs and were assessed through a combination of CSDT with 19 different models of effective shear width. In other analyses, the entire database with 214 test results 20 of slabs failing by different mechanisms was evaluated and a general effective shear width model was 21 proposed (GESW). The best results, which are a function of the effective shear width model used,

22 reached a mean ratio between experimental and predicted shear capacities of 1.06 with a coefficient 23 of variation of 14%, which is similar to that reported by some studies including linear and non-linear 24 finite element analyses. Furthermore, this level of accuracy was insensitive to the shear slenderness 25 and support conditions of the tests. The extended CSDT predicted the shear capacity of bridge deck 26 slabs in preliminary analyses more precise than semi-empirical models provided in the current design 27 codes, and the level of accuracy is comparable to methods using Linear Finite Element Analyses 28 (LFEA). Moreover, our proposed combination of the CSDT with a general effective shear width 29 model (GESW) provides reasonable levels of accuracy for slabs under concentrated loads regardless 30 of the failure mode of the tests. Therefore, the proposed approaches can be applied to bridge deck 31 slabs, which are subjected to a variety of loading and support conditions.

32 **Keywords**: Bridge deck slabs; Critical shear displacement theory; Database; Effective shear width;
33 Reinforced concrete; Shear strength;

34

35 **1 INTRODUCTION**

36 The shear capacity of bridge deck slabs attracted attention from several researchers and bridge 37 owners in Europe in the last decade since a large number of these structures built between 1960 and 38 1980 have reached the end of their originally devised service life [1–4]. A number of these bridges 39 do not rate sufficiently for shear according to the currently governing codes, despite no signal of 40 distress. This result indicated that widely accepted semi-empirical approaches of design could be 41 overly conservative. Since conservative predictions of shear strength could indicate the need for 42 replacement or retrofitting of these structures, the identification of more accurate approaches for 43 predicting the shear capacity of bridge deck slabs involves an economic and environmental issue, 44 beyond the user's safety. Apart from that, the design of wide reinforced concrete members prioritizes 45 solutions without shear reinforcement, since installing shear reinforcement is not cost-effective and 46 may result in reinforcement congestion. Therefore, also in design, the use of precise one-way shear 47 models can be essential to ensure adequate safety levels for members without stirrups.

48

49 Figure 1 - Slabs loaded (a) over the entire width analyses by de Sousa et al. [5] and b) under 50 concentrated loads in non-symmetrical conditions subjected to one-way shear failures.

51 In a previous study on wide beams and one-way slabs loaded over the entire width [5] (Figure 52 1a), it was identified that the Critical Shear Displacement Theory model (CSDT [6,7]) showed the 53 best levels of accuracy and precision compared to many semi-empirical and mechanical models of 54 shear strength, with the mean ratio between experimental and predicted shear capacities of 1.15 and 55 COV of 16%. Different from previous publications [8,9], de Sousa et al. [5] applied the analyses for 56 both slender and non-slender members, in addition to different support and loading conditions. 57 Therefore, it was decided to further assess the CSDT model for slabs under concentrated loads in 58 non-symmetrical conditions (Figure 1b), with emphasis on the one-way shear capacity.

59 Although the number of studies on shear in reinforced concrete members increased 60 significantly in the last decade, most of them were focused on the level of precision by semi-empirical

61 code models of shear strength [3,10–13]. In publications that include mechanical-based models [2,14–

62 16], the analyses focused on one kind of support conditions and hence, covered a reduced number of 63 tests. At the same time, only a limited number of studies addressed the fact the slabs under 64 concentrated loads may show a transitional failure mode between one-way and two-way shear [17]. 65 As a consequence, if the governing failure mode is unknown, the use of a one-way shear model to 66 assess members whose governing failure mode is punching shear may lead to unsafe predictions of 67 shear strength. Therefore, we identified the need for a more comprehensive study, covering slabs 68 under different support conditions, assessed by a mechanical-based model such as the CSDT and 69 accounting for different failure modes that may take place.

70 In this study, the application of the Critical Shear Displacement Theory Model (CSDT) [6,7] 71 is extended to the assessment of one-way shear capacity of wide reinforced concrete members under 72 concentrated loads in non-symmetrical conditions (Figure 1b). Different from previous studies, we 73 covered a variety of support conditions (cantilevers, simply supported and continuous members; 74 members under different loading conditions such as single loads and double loads close to the support; 75 and we provided recommendations when the governing failure mode is known or unknown.

76 The literature was reviewed in order to discuss the influence of the shear slenderness over the 77 governing failure mode of slabs. Furthermore, models to account the slab behavior under concentrated 78 loads and approaches to account improved shear capacities for loads close to the support are described 79 and assessed in the paper. Different databases were used to derive and validate each recommendation 80 for cases where the governing failure mode is known or unknown and how to account for the higher 81 shear strength for slabs under concentrated loads close to the support. The application limits and 82 benefits of each recommendation are highlighted in the paper, which also compares the results with 83 well-established models from the literature.

84 **2 LITERATURE REVIEW**

85 **2.1 Shear failure modes**

86 One-way shear failure and two-way shear failure or punching can be critical in bridge deck 87 slabs without shear reinforcement [2,17]. The critical failure mode can vary according to the gradient 88 of shear forces close to concentrated loads [18]. For slabs loaded over the entire width, the shear force 89 per unit length is almost constant over the shear span if the self-weight is neglected. On the other 90 hand, for flat slabs under concentric loads, the gradient of unitary shear forces (shear force per unit 91 length of the critical perimeter) becomes higher near the loaded region, since the perimeter of the 92 shear transfer is reduced [18]. Some studies suggest the combination of shear field analyses with one

93 way and two-way shear models for the determination of the critical failure mode [2,19], whereas 94 others already highlight that some tests can show the same capacity for one-way and two-way shear 95 [20]. This means that the ratio between the one-way shear effects (V_{exp}) from the acting punching load 96 (P_{exp}) with the calculated one-way shear capacity (V_{calc}) is very similar to the ratio between the acting 97 punching load (P_{exp}) with the calculated punching capacity (P_{calc}). Since the most critical failure mode 98 may change according to the geometry of the load, slab, and support conditions [14], the check of 99 both failure modes is essential for the assessment of existing structures, where a precise estimation 100 of the shear capacity is required [20].

101

102 Figure 2 - Critical regions of one-way and two-way shear for a) cantilever (adapted from Reiβen [21]
103 and b) simply supported members; c) effective width definition for one-way shear analyses (adapted
104 from Reiβen [21])

105 Figure 2 shows the complex transition between these two failure modes. For cantilever slabs 106 under concentrated loads, for instance, regions of critical one-way and two-way shear can be better 107 differentiated for large shear spans (Figure 2a), whereas for simply supported slabs, such regions

108 intercept each other (Figure 2b). Different studies have agreed on the existence of a trend for the 109 punching failure mode to become critical for higher shear slenderness [17,20–23].

110 Attention should be drawn to the fact that both one-way shear expressions and punching shear 111 expressions were derived and calibrated using lab tests designed with idealized boundary conditions. 112 For instance, one-way shear expressions were derived based on simply supported beam tests with 113 point loads [24]; and punching shear expressions were based on punching tests on idealized slab
114 column connections. One-way slabs typically have boundary conditions and failure modes between 115 the two types of failure modes, therefore, none of these two types of expressions were developed for 116 such structures.

117 **2.2 Effective shear width**

118 When slabs are subjected to concentrated loads, an effective shear width needs to be defined 119 together with a one-way shear model, since not the full slab width carries the same shear stress [2,25]. 120 Figure 2c shows the profile of shear stresses over the support as well as the distribution of shear 121 stresses around the load [2,3,22,25]. Integrating the shear stress v_{perp} over the width results in the 122 sectional shear at failure. However, for design, deriving the shear stress distribution over the support 123 is not practical, and therefore a uniform shear stress is commonly considered over a reduced width, 124 which is the effective shear width (Figure 2c). The integral of the maximum shear stress $v_{perp,max}$ over 125 the effective width should theoretically approach the integral of the shear stress v_{perp} over the full 126 width. The values of $v_{perp,max}$ can be determined by linear elastic finite element (LEFE) analysis with 127 shell elements adjusting the shear modulus G and the Poisson ratio v to account for cracking and load 128 redistribution [2,11,19,26,27]. However, the relevant section may vary according to the shear model 129 (between d and $d/2$ away from discontinuities or at the support) and according to the support and 130 loading conditions [20].

131 In practice, the effective width is usually defined based on a method of horizontal load 132 spreading from the concentrated load to the support or a section parallel to the support (Figure 3). 133 However, some publications already highlighted that the French method (as shown in Figure 3) could 134 overestimate the effective width in more than 30% for tests with shear slenderness higher than 5 [28].
135 Physically, this horizontal load spreading can be influenced by factors such as the reinforcement ratio
136 in the transverse direction [1,3], available member width [3,29], and size of the concentrated load 137 [21].

138
139 Figure 3 – Models of effective shear width used in design guides with respective reference lines. 140 Table 1 shows an overview of expressions for the effective width in the one-way shear strength 141 of reinforced concrete members under concentrated loads at the slab mid-width. For loads close to 142 the

edge, however, the effective shear width are equal to $b_r + b_{eff}/2$, where b_r is the distance from the 143 load axe to the free edge of one-way slabs. Table 1 displays some replaced design code models, e.g. 144 the Brazilian code from 1980 [30], since the current codes do not provide recommendations related 145 to the effective shear width. According to the table, most code provisions [30–34] and some proposed 146 in the literature [22,35,36] assume the effective width increases for larger shear spans. This idea relies 147 on the yield line theory [37] and experimental investigations [38], which account for shear forces 148 spreading on elastic plates under concentrated loads, also confirmed partially by LEFE analyses [2]. 149 In summary, most available models of effective shear width do not take into account the change in 150 the governing failure mode according to the position of the load [32,34] or were calibrated for specific 151 supporting conditions [15]. More consistent models of effective shear width, on the other hand, 152 usually require LEFE analyses [2].

153 Table 1 - Overview of analytical models that predict the effective width in analyses of one-way
154 shear strength of wide RC members under concentrated loads close to the support.

Old Dutch approach [31] (replaced)	$b_{eff} = b_{load} + 2 \cdot a_v$ (1)
French [32]	$b_{eff} = b_{load} + 2 \cdot a_v + (l_{load} - b_{load})$ (2)
Brazilian code [30] (replaced)	$b_{load} = b_0 + 2 \cdot h$ (3) For cantilever members: $b_{eff} = b_0 + 0.5 \cdot b_{slab} \cdot \left(1 - \left\lvert \frac{b_{NBR}}{b_{slab}} - 0.5 \right\rvert\right) \leq b_0 + 0.5 \cdot b_{NBR}$ (4) For other static systems: $b_{eff} = b_0 + 0.5 \cdot b_{slab} \cdot \left(1 - \left\lvert \frac{b_{NBR}}{b_{slab}} - 0.5 \right\rvert\right) \leq b_0 + 0.5 \cdot b_{NBR}$ (5)
German guideline [39] (replaced)	$b_{load} = t_{load} + 2 \cdot h$ (6) For cantilever members:

	$\begin{cases} + < < < < < \\ \end{cases}$ 0.2 0.3for: 0.2 ; t 0.2 ; t 0, 2 $b_{t\,a\,a\,t\,t} = \begin{cases} \\ + < < < < < < \end{cases}$ $a\ a$ $_{k\,k\,k\,y\,k\,x\,k}$ 0.3 for: 0.2 ; 0.2 0.4 ; 0.2 $_{240}^{H}$ $_{y\,k\,k\,k\,y\,k\,x\,k}$(7) For simply supported members: $_{240}$ 0.5 for: 0 , 0.8 , $_{H\,y\,y\,x}$ $b\ t\ a\ a\ t\ t = + < < \leq \leq$(8) For loads close to simple support of continuous members: $_{240}$ 0.4 for: 0.2 , 0.4 , 0.2 $_{H\,y\,y\,x}$ $b\ t\ a\ a\ t\ t = + < < \leq \cdot \leq$(9) For loads close to continuous supports $_{240}$ 0.3 for: 0.2 , 0.4 , 0.2 $_{H\,y\,y\,x}$ $b\ t\ a\ a\ t\ t = + < < \leq \leq$(10)
Swedish Code [40] (replaced)	$\begin{cases} + \cdot \\ \end{cases}$ $b\ d$ $_{load\ l}$ 7 $= \begin{cases} \\ \cdot + + \cdot \end{cases}$(11) $b_{b\,l\,d}$ $\max_{0.65\ 10.65}$ $_{BBK}$ ( ) $_{load\ load\ l}$
fib Model Code 2010 [34]	$b\ l\ b\ a\ d\ a_{effMC\ load\ load\ v\ l\ v} = + \cdot + - \cdot 2 \min ; / 2 \tan (( ))$ θ(12) 45º , cantilever of continuous members $\theta = \begin{cases} \\ \end{cases}$ 60º, if load is close to simple support
Zheng et al. [41]	$b\ l\ l\ r_{Zh\ load\ span\ cp} = + \cdot - \cdot \Phi (1 \tan)$(13) b $= \leq$(14) r_{l} 0.4 ^{load} $_{cp}$ $_{span}$ (º 23.3 35.1) $_{cp}$ $\Phi = \cdot + r$(15)
Bauer [35]	$_{eff\ Bauer\ load\ eff\ ,\ 1}$ $b\ l\ b = +$(16)
Vidaković and Halvonik [36]	For cantilever members: $b\ l\ b\ d\ a_{\ eff\ VH\ load\ load\ l\ v\ ,} = + \cdot + \cdot 2 \min 2 ; (( ))$(17)

Reiβen and Hegger [42,43]	For simply supported members: $b_{eff,b,q,l,a,d} = \cdot \cdot \cdot \cdot \lambda_b \lambda_\rho \lambda_l \lambda_{a,d}$ (18) $\lambda_b = -\cdot \leq \leq$ 1.2 0.12 1, for 5.5 $b_b \, m$ $\lambda_\rho = +\cdot \leq \leq$ 0.74 2.2 , for 0 0.7% $\rho_{q,q,q}^{0.4}$ (19) $\lambda_l = +\cdot \leq \geq$ 0.81 0.045 1.04 , for 2 $l_l \, m$ $\lambda_{a,d} = -\cdot$ 1.8 0.19 / for a_d $\lambda_{a,d} \leq \leq$ /, 2.91 / 5.41
Reiβen [21]	$_{\text{Reiβen}}, 7_{l,load,bf,load} b_d k_l = \cdot + \cdot$ (20) With: $d_{l,load} \leq 0.40$ m 5 9 1 $8 4 0.5^{bf} k_a a_d \lceil \leq = -\cdot + \rfloor \geq$ (21) max ; / , $( )_{1,2}$
Rombach and Velasco [44]	For LEFE analyses: $0.6 \; 0.95 \; 1.15_{RV} b_h a = +\cdot + \cdot$ (22)
Natário et al. [2]	For LEFE analyses on cantilever slabs: $_{eff,aplied,avg,d} b_F v =$ (23) $/_{,4}$
Shu et al. [45]	For NLFE analyses on cantilever slabs:

	$v_{E,avg}$ $= \cdot = \cdot \beta$ (24) ,

	b b b *v* *eff Shu w w w* , 1 *R code* ,

155

156

157 **2.3 Failure modes and shear transfer mechanisms in one-way shear**

158 Since Kani [46] and Leonhardt and Walther [47], it has been known that different shear failure 159 modes can occur as a function of the shear slenderness *M/Vd* and that shear strength increases 160 considerably for short members. Figure 4 shows the way the nominal shear strength of wide 161 reinforced concrete members (width-to-effective depth *b/d*>1) increases as the shear slenderness

162 decreases for tests under concentrated loads (CL) [5]. The figure also shows how the critical shear 163 crack shape changes according to the shear slenderness [48]. For concentrated loads close to the 164 support, or shear slenderness *M/Vd* < 2.5, direct load transfer may occur by compressive struts 165 improving the shear capacity. Such members are usually called non-slender members or deep beams 166 for beam-shaped members. The higher concentration of compressive stresses between load and 167 support usually leads to the crushing of concrete at failure [49]. This failure mode is called shear

168 compression failure [7].

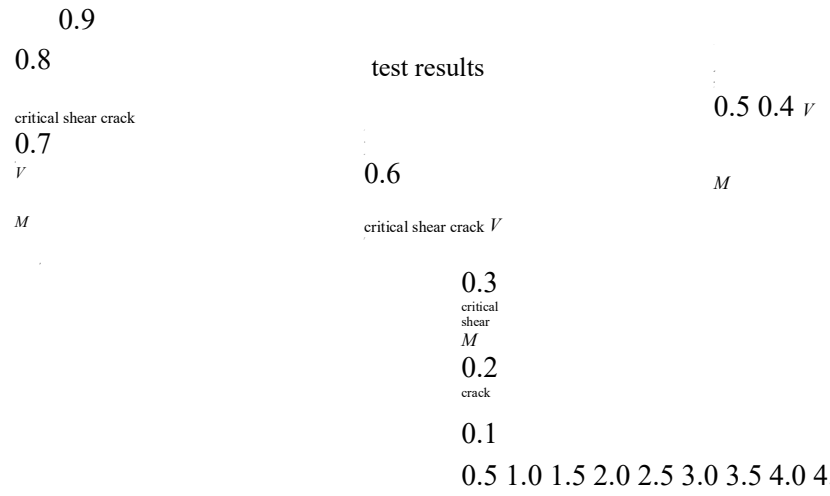

169

170 Figure 4 - Shear slenderness effect on the one-way shear behavior of wide reinforced concrete 171 members without stirrups. Adapted from de Sousa et al. [5].

172 Commonly, the same shear strength model derived for flexure-shear failures is used for the 173 design and verification of shear strength of non-slender members through the application of a factor 174 that reduces the acting shear force V_{Ed} or improves the shear capacity V_R in a critical section, as 175 suggested in NEN 1992-1-1:2005 [50] and *fib* Model Code 2010 [34]. The shear reduction factor β 176 from NEN-EN 1992-1-1:2005 [50] first considered only the bending moment effect on the 177 compression chord or cantilever action [51]. This means that only the effect of lower crack openings 178 and large compression chord depth were taken into account. In fact, the shear strength enhancement 179 for non-slender members is caused by a combination of the following mechanisms: (i) higher 180 compression chord capacity (cantilever action [18,51]) due to the large compression zone depth [49] 181 and (ii) direct load transfer that occurs by compression arch beyond the inclined cracking load (or

182 strut if it has a straight shape), also named arching action [17,52]. In the literature, both mechanisms
183 are cited as the source of improved arching action [2].

184 Table 2 shows a summary of the main expressions suggested by different references to account 185 for the increase in shear capacity for loads close to supports – past codes used the shear span to depth 186 ratio *a/d* as the main parameter. The model proposed by Reiβen [21] was calibrated for the European 187 code shear model and took into account the ratio $max\{a_1;a_2\}/d$ (a_1 and a_2 refer to the distances from 188 the section of zero bending moment to the support and load axes, respectively) in such a way that it 189 provides precise estimations of strength for both simply supported and continuous members. In this 190 text, the ratio $max\{a_1;a_2\}/d$ has the same meaning as the shear slenderness M/Vd. Since the influence 191 of the shear slenderness is already taken into account in the shear models from *fib* Model Code 2010 192 and SIA 262:2013 by the calculations of the internal forces, the β factor takes into account the 193 improved arching action only by the clear shear span-to-effective depth ratio a_v/d as a more 194 conservative approach.

195 Table 2 - Expressions for reducing the acting shear load V_E for non-slender members according to 196 different references.

Reference	Model
ABNT NBR 6118:2014 [53] – Brazilian code DIN 1045:1988 [54] – German code	$\beta = \frac{a}{2d}$ (25)
DIN 1045-1:2001 [55]– German code	$\beta = \frac{x}{2d}$ (26) x measured from load axis to support edge
NEN-EN 1992-1-1:2005 [50] – European code	$\beta_{EC} = \frac{a_v}{2d} \geq 0.25$ (27) $\beta \leq 1.00$
fib Model Code 2010 [34]	$\beta = \frac{a_v}{2d} \geq$ (28) $\beta \leq 1.00$

	$\beta_{MC} = \frac{2}{1 + 50\,d}$
SIA 262:2013 [56] – Swiss code	$\beta_{SIA} = \frac{a_v}{2\,d} \geq 0.25$ (29)
Reiβen [21]	$\beta_{R16} = \frac{2.8}{1 + 0.4\,d} \leq \max\{a_1; a_2\} \geq 1.0$ (30)
Natário et al. [2]	$\beta_{Nat14} = \frac{2.75}{1 + 0.50\,d} \leq a_v \geq 1.00$ (31)
Yang et al. [57]	$\beta = \frac{M}{M - V_d d_{Vd}} \leq \frac{2}{1 + [\varepsilon_x / 0.1]}$ (32)

197

198 **2.4 Critical Shear Displacement Theory Model**

199 The Critical Shear Displacement Theory (CSDT) [6,7] assumes that a critical inclined crack 200 starts from a major flexural crack, which will lead to collapse when the shear displacement Δ of the 201 crack reaches a critical value and causes a secondary crack (dowel crack) along the reinforcement. A 202 dowel crack causes the detachment of the tensile reinforcement from the concrete along the shear 203 span, which significantly reduces the lateral confinement on the crack and the member flexural 204 stiffness [7]. Due to

the opening of the main crack, an additional vertical shear displacement is 205 required for the recovery of the previous shear stress level in the crack, which feeds the growth of 206 flexure-shear cracks and leads to a brittle collapse of the member [7].

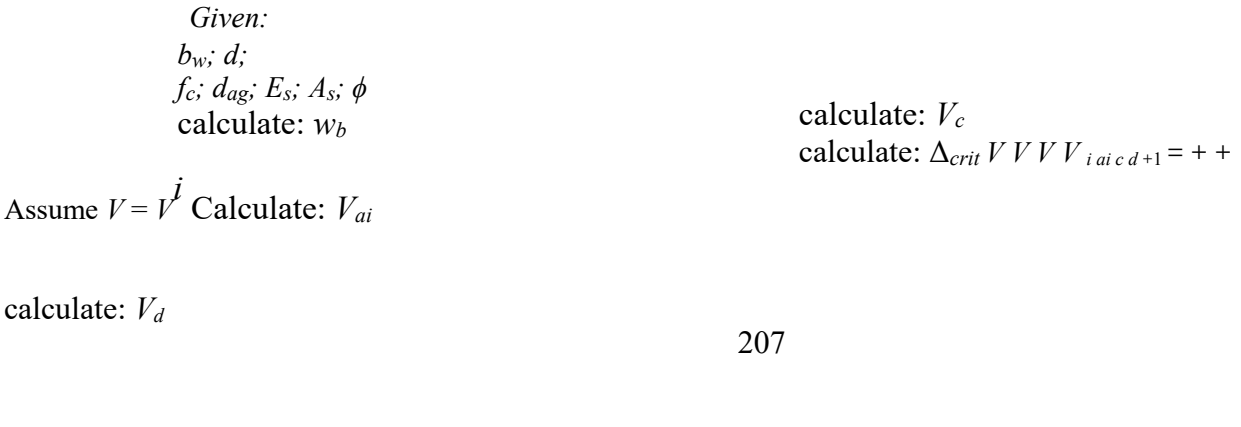

208 Figure 5 - Flowchart of the calculations using the CSDT model

209 The CSDT assumes that the shear capacity of RC members without stirrups is resisted by (i) 210 compression chord capacity [58], (ii) dowel action [59], and (iii) aggregate interlock [60]. The 211 contribution of the residual tensile strength of concrete is neglected at failure [7], and the aggregate 212 interlock contribution is a function of the crack width w_b at the level of the tensile reinforcement and 213 derived from the shear displacement Δ [61]. Figure 5 and Table 3 show, respectively, a flowchart of 214 the calculations for the prediction of shear capacity and the base equations used.

215

216

217

218

12

219 Table 3 – Expressions used in the CSDT [6]

Model	**Expression**
General [6]	$V_{u} = V_{c} + V_{ai} + V_{d}$ (33)
Compression chord [58]	$V_c = \frac{z}{2} \frac{d_s}{}$ (34)

	$V V V$ $c\ cr$ c 3 $z\ d\ s$ cr
Aggregate interlock [6]	⌈ Δ − Δ ⌉ ⌉ ⌋ $R\ b\ A\ w\ A\ w\ ds$, , s ∫ (( ) ( )) $ai\ pu\ x\ y$ cr σμ 0 $V\ R\ f\ s\ b_{w}$ = − Δ + Δ − ⌋ − ⌋ 0.03 either of 978 ² 85 0.27 ( ) 0.56 $ai\ ai\ c\ cr$ (35) 0.01 b $R\ w\ bds$ ⌈ Δ ⌉ ⌊ s ∫ ( ) $ai\ ai$ cr τ , 0
Dowel action [59]	= φ(36) ^{3} 1.64 , in [MPa] $V\ b\ f\ f_{d\ n\ c\ c}$
Factors	**Expression**
Height of fully developed crack	(( ))^{2} 1 2 $_{cr\ l\ e\ l\ e\ l\ e}$ $s\ n\ n\ n\ d$ = + − + ρ ρ ρ(37)
Critical shear displacement	25 0.0022 0.025 mm d Δ = + ≤(38) 30610 ^{cr} φ
Crack width at the bottom of the crack	M =(39) $w\ l$ $b\ cr\ m,$

	$zA\,E$ $s\,s$
Reduction factor for aggregate interlock for high strength concrete [6]	$R_f = \cdot \left(\frac{7.2}{40\,a_i}\right)^2 + \left(0.85 - \frac{1}{1 - 0.34}\right)$ with f_c in MPa and $f_c > 65$ MPa (40)

220

221

222

223 **3 DATABASES**

224 This study assumes that checking both shear-critical failure modes, one-way and two-way 225 shear, is essential to identify the governing failure modes of existing bridge deck slabs. Therefore, a 226 careful classification of the failure modes of tests from the literature is of paramount importance to 227 understand the limits of application of the available one-way and two-way shear models. Moreover, 228 this classification allows a fairer assessment of the precision of one-way and two-way shear models, 229 as well as models of effective shear width for slabs under concentrated loads.

230 This study will discuss the results of three database subsets which are published in the public 231

domain [62]: (i) wide beams and one-way slabs loaded over the entire width failing in one-way shear 232 (Database A); (ii) slabs under a single concentrated load failing in one-way shear, two-way shear or 233 a combination of both (Database B0) and; (iii) slabs subjected to double loads close to the line support 234 (Database C).

235 **3.1 Database filtering and organization**

236 The Database B0 includes 214 test results of slabs under single concentrated loads that were 237 classified according to the main failure mode in (i) wide beam shear or one-way shear (WB), (ii) 238 punching shear (P) and (iii) transition mode between wide beam shear and punching shear (WB/P). 239 Since this study focuses on the one-way shear model, tests with signs of punching failure were 240 initially removed from the database B0, which resulted in the database B1 (141 tests). This filtering 241 was based on (i) the cracking pattern of the members, when available in the original references and 242 (ii) the classification reported by other authors [10,63], which was also based on the cracking pattern

243 and (iii) in the classification of Natário [20], who combined shear fields from LEFE analyses with 244 one-way shear and punching shear models according to the Critical Shear Crack Theory (CSCT) 245 [2,19,20]. The main criteria used for the removal of members because of a punching failure in this 246 study were (i) absence of a critical shear crack visible on the edge of the members and (ii) position at 247 which the critical shear crack intercepted the middle depth of the member when the cut view was

248 available. When the internal cracking pattern was not shown in the references, it was considered a 249 punching failure if the cracking pattern was predominantly formed by radial and tangential cracks or 250 if a conical crack could be seen.

251 The database B1 of slabs under concentrated loads after removing punching tests 252 comprehends 141 test results from the following references: Cullington et al. [64], Lantsoght [63], 253 Reiβen [21], Lubell [65], Bui et al. [66], Regan [67], Regan and Rezai-Jarobi [68], Vaz Rodriguez 254 et al. [69], Rombach and Latte [70,71], Natário et al. [2,72], Rombach and Henze [73], and Vida et 255 al. [74]. The database entries include the effect of self-weight on the calculated shear capacities and 256 on the shear slenderness parameters for continuous members.

257 The database B1, whose organization was inspired by those of Lantsoght et al. [10], Reiβen 258 [21] and Henze et al. [11], has been published in the public domain [62] and includes 46 tests on 259 cantilever members (CT), 33 tests with concentrated loads close to the internal support of continuous 260 members (CS), and 62 tests with concentrated loads close to the simple supports (SS). It also includes
261 two modes of one-way shear failures, namely shear-compression failures for non-slender members, 262 or shear slenderness $M/Vd < 2.5$ (55 tests ≡ 39 %), and flexure-shear failures for slender members, or 263 shear slenderness $M/Vd \geq 2.5$ (86 tests ≡ 61%).

264 Figure 6 displays the main geometrical loading parameters in the database for members with 265 continuity over line supports and subjected to a combination of concentrated loads and line loads. 266 The same definitions have been used for other structural systems.

267

268 Figure 6 - Geometrical parameters of wide members with continuity over the support. 269 Figure 7 shows the distributions of the parameters related to the tests included in the database 270 B1. Similar to beam-databases [75,76], most experiments were performed for members of thicknesses 271 less than 600 mm (Figure 7a) and on wide members whose ratio between the slab width and load 272 dimensions in the width direction was higher than 5 (Figure 7b). The full width of members with 273 $b_{slab}/l_{load} < 5$ was probably activated in the test, depending on the distance from the load to the support. 274 However, as some models of effective width are overly conservative, some predictions may indicate 275 that the full width was not mobilized. Figure 7c shows that the b_{slab}/h aspect ratio (Figure 11c) was 276 higher than 5 in more than 75% of the tests, and Figure 7d highlights the number of tests in the 277 database performed

with a shear slenderness *M/Vd* between 2 and 3. This range indicates that a considerable number of tests were subjected to a transitional failure mode between shear-compression and flexure-shear. Figure 7e show that 16 tests from the database have a concrete compressive strength larger than 60 MPa and, hence, the level of accuracy for members with reduced aggregate interlock may be assessed. Figure 7f shows that the longitudinal reinforcement ratio ranges between 0.6 and 1.8%, where the larger ratios may not be representative of those used in bridge deck slabs.

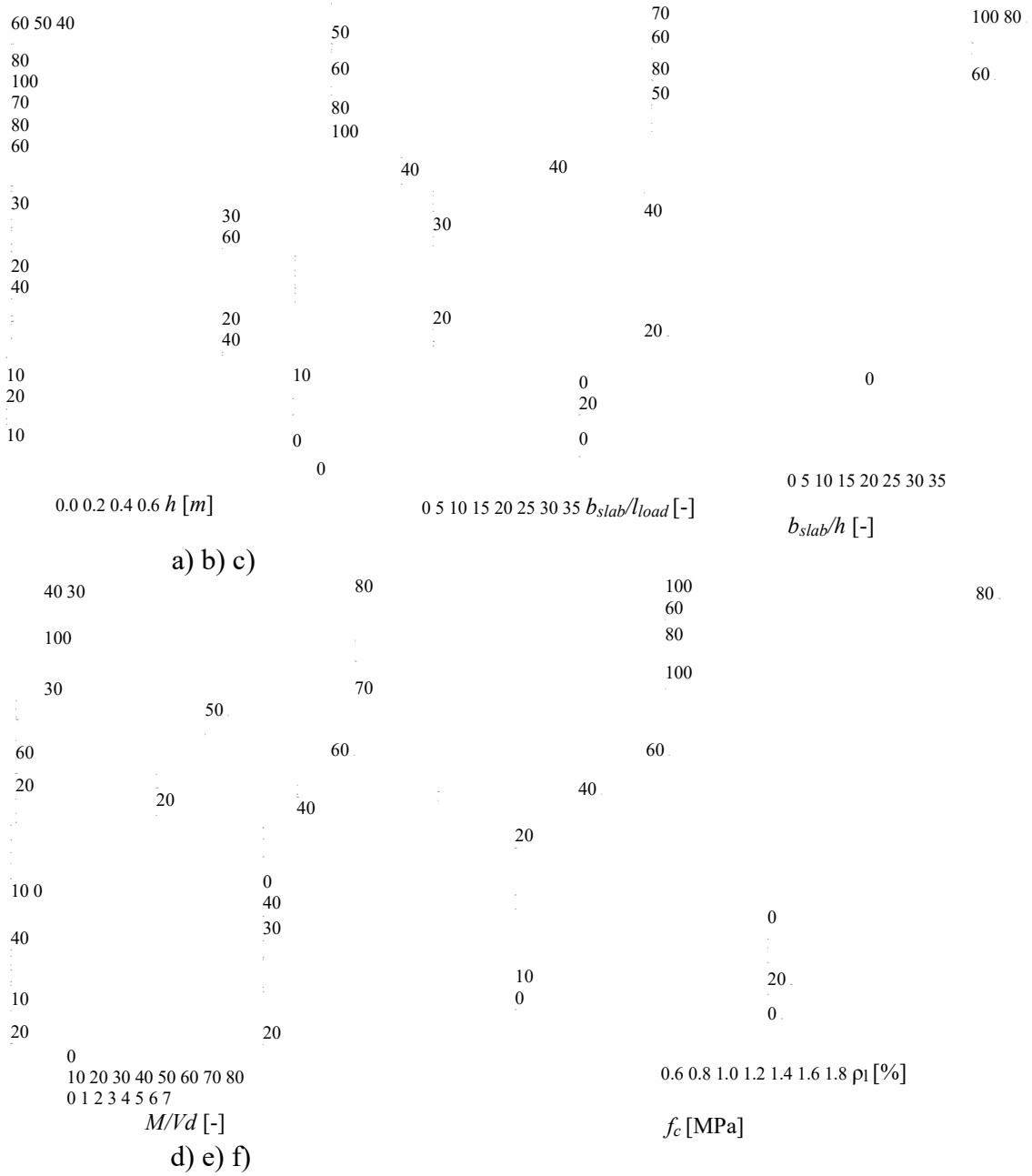

Figure 7 – Distribution of parameters in the database B1 for the following parameters: a) thickness

of the slab at the support edge, b) ratio of slab width-to-load dimension in the width direction, c) ratio 285 of slab width-to-effective depth, d) shear slenderness; e) concrete compressive strength and f) 286 longitudinal reinforcement ratio.

287 **4 PROPOSED RECOMMENDATIONS**

288 **4.1 Section for internal forces calculations**

289 Since most mechanical based models of shear strength were derived for shear slenderness 290 M/Vd higher than 2.5, the assumption of the section far from d or $d/2$ from the highest bending 291 moment axes [6,77] or from geometrical discontinuity [34] does not play an important influence. 292 However, when using these models for lower slenderness ($M/Vd < 2.5$), the location of this section 293 assumes a major influence. Because of this, a previous investigation was made in order to identify 294 the section that could balance precision and safety for the ratio V_{exp}/V_{cal} in both ranges of shear 295 slenderness and for different support conditions (Figure 8b,c,d). Assuming that the shear capacity is 296 reduced due to an increase in the opening of the critical shear crack [6,77,78], the control section for 297 the calculations of the internal forces M_{Ed} and V_{Ed} remain at sections close to the higher bending 298 moment for all models. However, the critical section at the support edge of cantilever slabs was used 299 instead of the section at d or $d/2$ from the support edge in order to reach better predictions for these 300 support conditions [5].

301

302 Figure 8 – a) reference lines to calculate the effective shear width in French model [32] and 303 proposed approach; critical sections used for b) cantilever members, c) simply supported members, 304 and d) continuous members.

305 **4.2 Arching action**

306 This study proposes to combine the CSDT result with a semi-empirical coefficient β based on 307 the ratio a_v/d (Equation (41)) to extend the CSDT model to predict the shear capacity of non-slender 308 members without additional iterative calculations:

$$\beta = \begin{cases} \dfrac{a_v}{1.00} & \leq \\ 1.00 & \geq \end{cases} \quad \begin{matrix} 18 \\ . \\ 2.5\ 0.40\ d \end{matrix} \qquad \text{Prop}$$

309 (41)

310 The combination of the CSDT with reduction factor β for non-slender members should be 311 understood as an engineering approach comparable to empirical simplifications used by most design 312 codes [34,50] and strain-based models [2]. Theoretically, this approach is not exact because the shear 313 failure mechanism for non-slender members is different from that for slender ones: the shape and 314 relative contribution of the main shear-transfer mechanisms vary significantly when the shear 315 slenderness decreases since the vertical branch of the assumed crack profile of the critical shear crack 316 becomes not representative anymore (Figure 9b).

317

318 Figure 9 - a) and b) Crack profile simplification for specimens with $M/Vd > 3$, c) main 319 parameters of CSDT, and d) crack profile for non-slender members ($M/Vd < 2$).

320 For lower shear slenderness, the inclination of the major flexural crack increases in such a 321 way that the contribution of the aggregate interlock decreases significantly, while the contribution of 322 the compression chord V_c increases according to internal equilibrium [79]. The use of strut-and-tie 323 models for continuous members with maximum shear slenderness $M/Vd < 2$ may better represent the 324 problem [80]: plane sections do not remain plane, and shear strains become dominant for those 325 members [81]. However, this approach may not be practical for the slabs studied since the problem 326 is strongly three-

dimensional. As such, for practical purposes, we consider the choice of including β 327 as adequate.

328 **4.3 Effective shear width**

329 In design and assessment of existing structures, two kinds of analyses may occur (i) the 330 governing failure mode is unknown, and a conservative prediction of the shear capacity may be 331 adequate for preliminary design, and (ii) a more precise estimation of the shear capacity is required, 332 usually in the assessment of existing structures preliminarily rated as critical in shear [82]. In the latter
333 case, a detailed analysis of the governing failure mode would be essential to determine the shear 334 capacity, which requires LEFE analyses combined with a mechanical-based model, such as conducted

335 by Natário [20] or using one-way and two-way shear models adjusted to slabs under concentrated 336 loads in non-symmetrical conditions.

337 Since the governing failure mode of the tests in the database B1 is known, we proposed in this 338 study two kinds of analyses. The first group of analyses investigatesthe accuracy of different effective 339 shear width models combined with the CSDT model using a database with the governing failure mode 340 known (one-way shear – Database B1). From these analyses, we derive recommendations for the
341 assessment of existing structures when the governing failure mode is known (one-way shear), and 342 precise estimation of the shear capacity is the main purpose.

343 The second group of analyses aims to assess the shear capacity of slabs when the governing 344 failure mode is unknown (Database B0). This means that one-way or two-way shear failures were 345 included in the analyses. In order to provide consistent predictions of shear capacity regardless of the 346 critical failure mode and covering different support conditions, the General Effective Shear width 347 model (GEWS) was developed accounting that if punching failure governs, the predicted one-way 348 shear capacity should be decreased by predicting a smaller effective shear width.

349 The idea of the GESW model is to provide a simple alternative to assess the shear capacity of 350 slabs using only a one-way shear model combined with an effective shear width. The proposed model 351 is based on the French effective shear width model [32] adjusted by a correction factor α. This factor 352 considers that increasing the shear slenderness ($\lambda=M/Vd$) or decreasing the effective depth of the 353 reinforcement, the punching shear failure becomes governing. Therefore, a reduced effective shear 354 width should be predicted for slabs on which punching shear may be critical. The values of α were 355 derived based on regression analyses to improve the average and coefficient of variation of the ratio 356 V_{exp}/V_{calc} with the CSDT model combined with the French model of effective shear width. These 357 regression analyses were organized according to the support conditions of the tests (Figure 10).

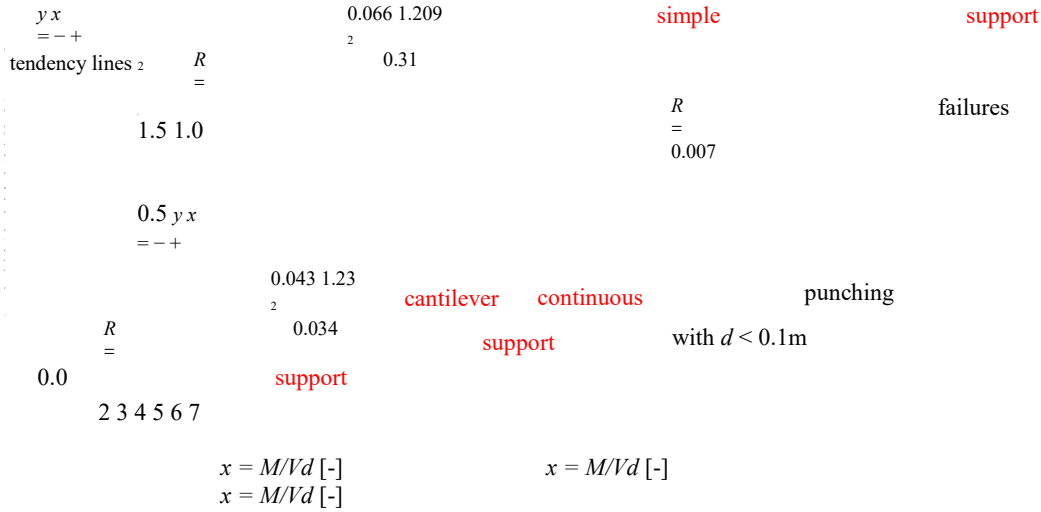

359 Figure 10 - Ratio of V_{exp} / V_{cal} of the CSDT combined with the original French effective shear width
360 model and $\beta_{proposed}$ to account improved arching action for loads close to the support.

361 Based on the literature review (Section 2) and parameters influence of V_{exp}/V_{cal} according to 362 the Database B0 similar to showed in Figure 10, we identified that the shear slenderness parameter 363 M/Vd would be the most important parameter to be considered in the GESW for all support 364 conditions. Table 4 shows the equations for the proposed model of effective shear width. Figure 8a 365 and Figure 11 illustrates this idea for simply supported slabs of small thickness. In Table 4, we 366 considered the effective depth d only for simply supported members by two reasons: (i) the thickness 367 variation is small in the database for other support conditions and (ii) to improve the predictions of 368 tests with punching failure and effective depth lower than 0.1 m (Figure 10). At this point, we 369 highlighted that this approach seeks to provide a model for design or preliminary assessment of 370 existing structures. When higher levels of approximation are required, the use of one-way and two
371 way shear models is essential to determine the governing failure mode, as we will discuss in the next
372 sections.

373 Table 4 - General effective shear width model proposed (GESW) according to the support conditions,
374 shear slenderness $\lambda=M/Vd$, and effective depth d of the longitudinal reinforcement.

General model	$b_{GESWM\ eff\ French}$ (42)
Cantilever slabs	$b_{GESWM\ eff\ French} = 1.05 - 0.05\lambda$ (43)
Simple support	$b_{GESWM\ eff\ French} = d + 1.08\lambda - 0.103\lambda^{2} - 0.31$ (44)
Continuous support	$b_{GESWM\ eff\ French} = 1.08 - 0.072\lambda$ (45)

375

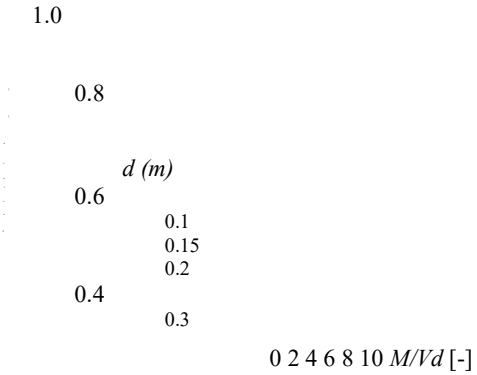

376

377 Figure 11 – Variation of the factor α according to the shear slenderness and effective depth of 378 reinforcement for the simply supported slabs.

379 **5 RESULTS**

380 This section addresses a comparison between the experimental shear strengths from the 381 databases A, B0, B1 and C [62], and those predicted by the CSDT model. Firstly, the level of accuracy 382 (average value - AVG) and precision (coefficient of variation - COV) of the V_{exp}/V_{cal} ratio for a 383 database of wide members loaded over the entire width was assessed according to the shear 384 slenderness, with no influence of the effective shear width model (Database A -Section 5.1). In a 385 second step, the analyses involved the database of slabs under single concentrated loads failing in 386 one-way shear (Database B1 - Sections 5.2, 5.3 and 5.4). Then we compared the predicted one-way 387 shear capacities with the experimental ones for 8 tests of slabs subjected to double concentrated loads 388 parallel to the support (Database C - Section 5.5). Finally, we discuss the results of analyses conducted 389 for the overall database of slabs under single loads (Database B0- Sections 5.6) using one-way and 390 two-way shear models.

391 **5.1 Members loaded over the full width – Proposal for $\beta_{arching}$**

392 This analyses aims to assess only the proposed model regarding the improved arching action 393 for non-slender members, without the influence of the effective shear width models. For this study, a 394 database of wide beams and one-way slabs loaded over the entire was used (Database A). This 395 database is published in the public domain [62] and covers different support conditions and a 396 comprehensive range of shear slendernesses. The database includes 36 tests with $M/Vd \leq 2.5$ and 146 397 tests with $M/Vd >$ 2.5.

398 Figure 12 shows a β factor derived based on a regression analysis with exponential adjustment 399 according to the shear slenderness $\lambda=M/Vd$. This graph highlighted that the scatter between predicted 400 and calculated shear strengths in the range of shear slenderness lower than 3 is considerably higher 401 compared to the other range. This occurs because the arching action is highly influenced by the 402 cracking pattern, which shows a higher variability for short slenderness [57]. Since the CSDT model 403 already takes into account the shear slenderness by the calculations of M_{Ed} and V_{Ed}, the β factor based 404 on the ratio M/Vd could lead to overly optimistic predictions of resistance, mainly when arching 405 action does not play an influence as a result of the occurring cracking pattern (see test without arching 406 action in Figure 12). Because of this, some authors proposed to adopt the inclined cracking load 407 instead of the ultimate shear load as the failure criterion since this parameter shows a considerably 408 lower scatter [57]. However, as most references do not report the inclined cracking load for slab tests 409 as this cracking is harder to observe in slabs under concentrated loads than in beam members, the 410 ultimate shear load was considered in the regression analyses.

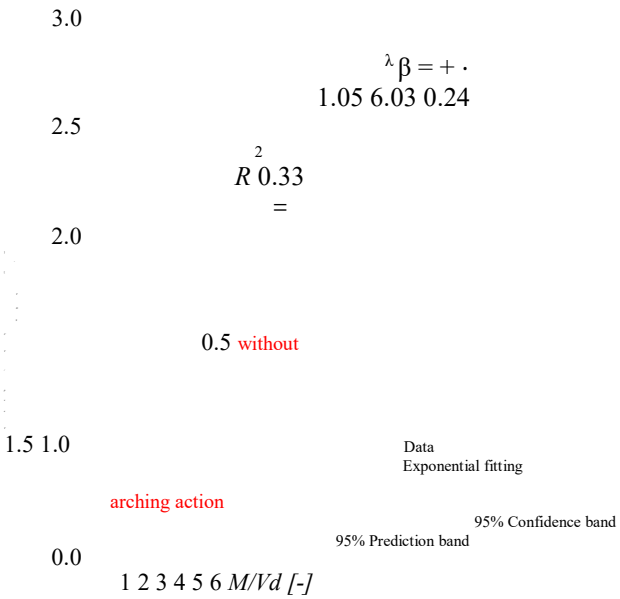

411

412 Figure 12 – Alternative β factor derived based on exponential fitting between experimental and 413 predicted shear strengths. Note: $\lambda = M/Vd$.

414 Figure 13 shows the V_{exp}/V_{calc} ratio according to the shear slenderness by including or not 415 different approaches for improved arching action for non-slender members. The gray ranges represent 416 ±1 standard deviation from the mean value.

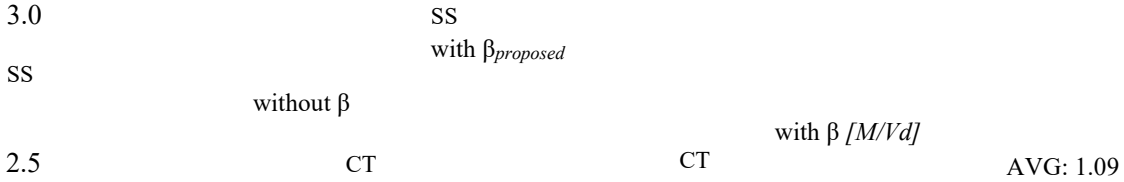

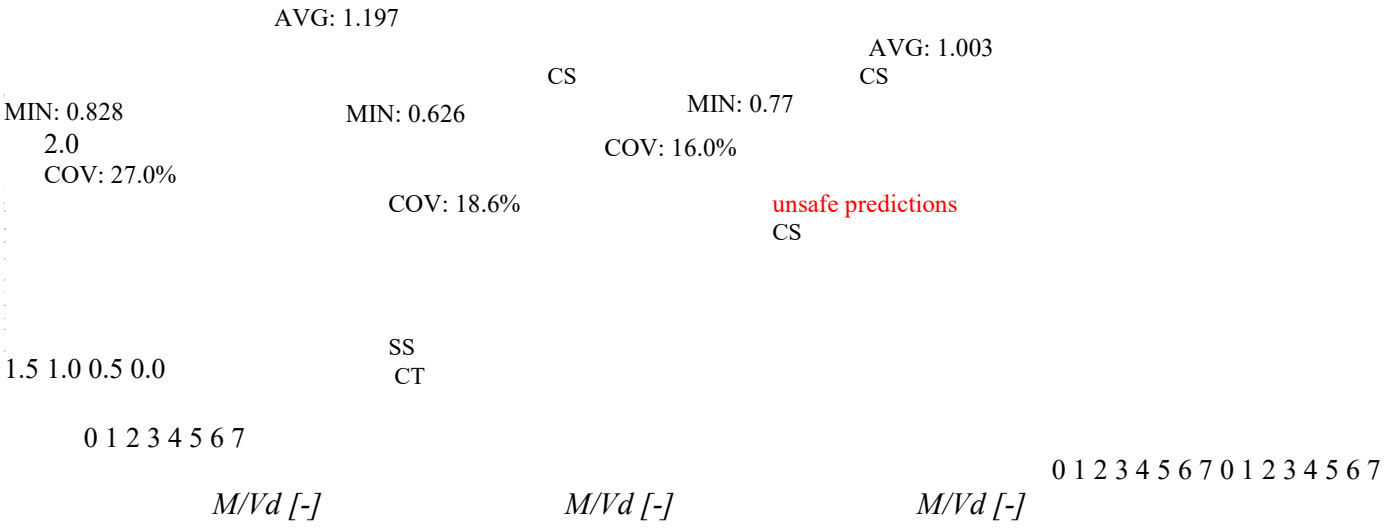

417

418 Figure 13 - Effect of factor β on the statistics of V_{exp}/V_{cal} for tests loaded over the entire width (line 419 loads). (CS = continuous support; CT = cantilever support and SS = simple support).

420 According to Figure 13, applying an improved arching action factor with the CSDT reduces 421 the coefficient of variation from 24.7% to 18.6% when using $\beta[M/Vd]$ (Figure 12), and to 16.0% when 422 using $\beta_{proposed}$ (Equation (41)). Any approach shows a wider scatter between experimental and 423 predicted shear capacities for continuous members (CS), due to the higher variability in the position 424 of the critical shear crack. Although the theoretical critical section was at $d/2$ from the position with 425 the maximum bending moment, this procedure is still conservative for most tests. Table 5 shows that 426 the average (AVG) V_{exp}/V_{cal} ratio ranged from 1.197 to 1.093 with the proposed factor β_{prop}. In Table 427 5, $V_{exp,red}$ refers to the experimental shear capacity reduced by the different parameters β. The lower 428 scatter between experimental and predicted shear capacities occurred with the $\beta_{proposed}$ and β_{EC}.

429 Table 5 - Statistical results of the predicted to calculated shear strengths according to different
430 approaches to account the arching action for non-slender members.

	$\frac{V_{exp}}{V_{CSDT}}$	$\frac{V_{exp,red}}{V_{CSDT}}$	$\frac{V_{exp,red}}{V_{CSDT}}$	$\frac{V_{exp,red}}{V_{CSDT}}$
Approach	*Without* β	*With* β_{EC}	*With* $\beta_{Figure\ 12}$	With $\beta_{proposed}$
AVG	1.197	1.134	1.003	1.093
MIN	0.828	0.828	0.626	0.770
COV	0.270	0.172	0.186	0.160

431

432 **5.2 Effective shear width models**

433 The database B1 gathered according to the descriptions in Section 3 [62] was used in the next 434 analyses of the level of accuracy of the CSDT combined with different approaches for the effective 435 shear width. Table 6 and Table 7 show statistical results from the V_{exp}/V_{calc} ratio for different ranges 436 of shear slenderness $\lambda=M/Vd$. The results are shown as a function of the ratio M/Vd instead of the 437 ratio a_v/d since the former is a more useful parameter to distinguish members subjected to shear
438 compression failure from those subjected to flexure-shear failures, mainly for continuous slabs. 439 $\beta_{proposed}$, which accounts for improved arching action for non-slender members, was adopted in most 440 analyses. Since some tests did not fulfill conditions related to load dimensions for use the effective 441 width from the German guidelines[39], Equations (6) to (10) in Table 1, this model was not evaluated.
442 In the same way, the model provided by Halvonik et al. [15] was not evaluated since this was purposed
443 only for cantilever specimens.

444 According to Table 6, older design code models of effective shear width, such as the Brazilian 445 model [30], lead to overly conservative predictions in most cases (mean $V_{exp,red}/V_{CSDT}$ = 1.772). The 446 Swedish provisions [40], on the other hand, lead to unsafe predictions, with average ratios of V_{exp}/V_{cal} 447 of 0.706 and 0.981 in the different ranges of shear slenderness evaluated. The *fib* model of effective 448 shear width leads to average values of V_{exp}/V_{cal} of 1.092 and 1.192 for non-slender and slender 449 members, respectively. The best accuracy and precision over the different slenderness ranges assessed 450 were achieved by the French model of effective shear width [32], thus indicating, on average, that the 451 French approach provides reasonable predictions of effective shear width for slabs failing in one-way 452 shear.

453

454 Table 6 - Statistics of V_{exp}/V_{calc} according to the range of shear slenderness $\lambda = M/Vd$ and effective
455 width model provided in design codes.

b_{eff}		ABNT	Swedish	French	*Fib*	λ	N	$\beta_{arching}$	$\frac{V_{exp,red}}{V_{CSDT}}$ Prop	$\frac{V_{exp,red}}{V_{CSDT}}$ Prop	$\frac{V_{exp,red}}{V_{CSDT}}$ Prop
		AVG	1.401	0.706	1.044	1.092					
		MIN	0.869	0.481	0.773	0.758					
		COV	21.9%	23.5%	11.4%	20.8%					
		AVG	2.009	0.981	1.070	1.192					
		MIN	0.818	0.438	0.723	0.513					
		COV	40.8%	18.7%	15.8%	23.7%					
		AVG	1.772	0.873	1.060	1.153					
		MIN	0.818	0.438	0.723	0.513					
		COV	41.2%	25.4%	14.3%	23.0%					
		456									
		457									
		<2.5	55	≥2.5	86	All	141				

458 Table 7 - Statistics of V_{exp}/V_{calc} according to the range of shear slenderness $\lambda = M/Vd$ and effective
459 width models suggested in the literature.

	$V_{exp,red}/V_{CSDT}$	V_{exp}/V_{CSDT} Reissen	$V_{exp,red}/V_{CSDT}$ Bauer	V_{CSDT} Prop (GESW)
b_{eff} Zheng				
λ N $\beta_{arching}$ Prop - Prop Prop	AVG 0.755 1.601 1.401 1.043			
MIN 0.512 1.113 0.869 0.748		AVG 1.089 1.624 1.772 1.197		
COV 22.7% 17.7% 21.9% 12.2%		MIN 0.459 0.983 0.818 0.748		
AVG 1.302 1.638 2.009 1.295		COV 41.3% 25.7% 41.2% 20.3%		
MIN 0.459 0.983 0.818 0.830		460		
COV 34.0% 29.6% 40.8% 19.2%		< 2.5 55 ≥ 2.5 86 All 141		

461 Table 7 shows that the average value of V_{exp}/V_{cal} ranged from 1.089 to 1.772 with the 462 approaches studied for the definition of an effective shear width. The effective width from Zheng et 463 al. [41] provided a wider scatter between experimental and predicted shear capacities (COV > 30% 464 on average) and a V_{exp}/V_{cal} mean value much lower than 1 for non-slender members. Since the 465 approach of Reiβen [21] includes the effect of the improved arching action on non-slender members 466 in the effective width model by using the factor k_{bf}(Equation (21) in Table 1), the experimental shear 467 capacities were not reduced for these calculations. The model provided conservative predictions of

468 shear strength for all tests assessed and a 25.7% coefficient of variation. Bauer and Muller's approach
469 [83] resulted in the most conservative predictions for slender members (V_{exp}/V_{cal} = 2.009), but with a
470 wider scatter (COV = 40.8%). The proposed GESW model provided good AVG (1.197) and COV 471
(20.3%) values compared to the other models. Comparing Table 6 and Table 7, both GESW model 472 and
French model provide an accurate estimation of the test results. However, the GESW turns out 473 to be
slightly more conservative for Database B1 as it was derived to assess slabs under both failure 474 modes
(one-way shear and two-way shear).

475 **5.3 Sensitivity of parameters**

476 Since the first purpose is to derive recommendations for precise predictions of shear strength 477 when the one-way shear failure mode is governing (Database B1), the CSDT combined with the 478 French effective shear width model and β_{prop} was further assessed with parameter studies (Figure 14).

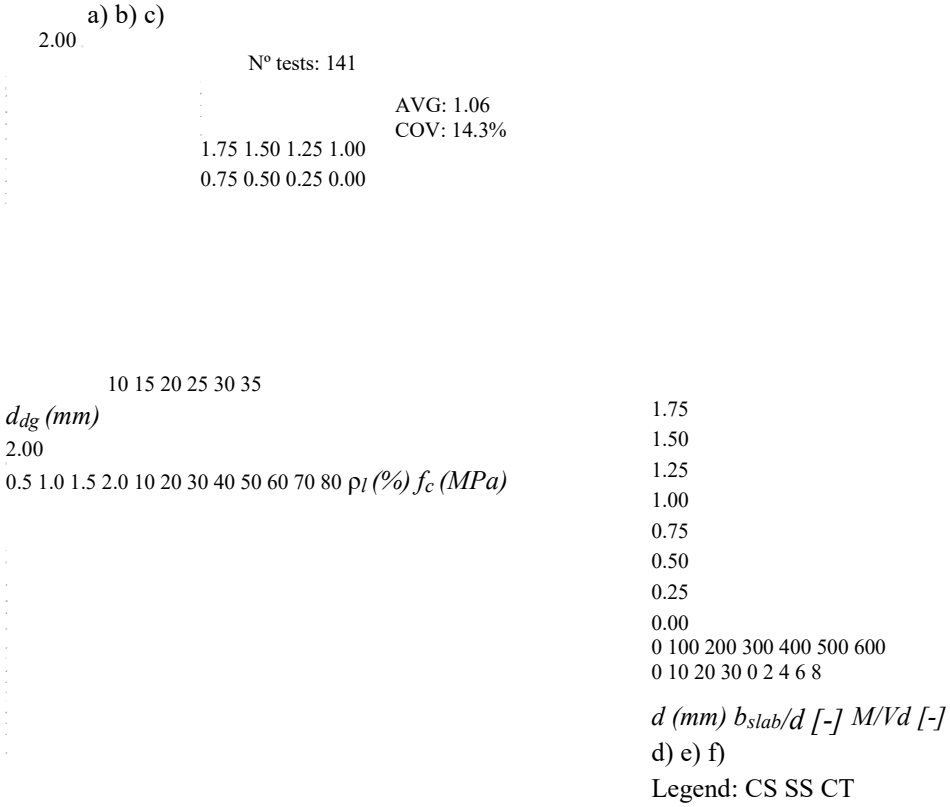

479

480 Figure 14 - V_{exp}/V_{cal} ratio as a function of the main mechanical and geometrical parameters for wide 481 members subjected to concentrated loads close to the support with predominant one-way shear 482 failure: a) aggregate size d_g, b) longitudinal reinforcement ratio ρ_l, c) concrete compressive strength 483 f_c, d) effective depth d, e) width-to-effective depth ratio b/d, and (e) shear slenderness M/Vd. (CS = 484 continuous support; CT = cantilever support and SS = simple support).

485 Figure 14 shows the ratio of $V_{exp,red}/V_{cal}$ as a function of different parameters. The results 486 indicate no significant influence of the aggregate size (Figure 14a) and reinforcement ratio (Figure 487 14b) on the predictions of shear strength with the studied approach. Wider scatter in some regions 488 (see Figure 14a) for 16 mm aggregate size can be assigned to a higher number of tests. Figure 14c 489 shows that the CSDT provides accurate and precise predictions of shear strength for members of high 490 strength concrete ($f_c >$ 65 MPa), for which a lower contribution of the aggregate interlock is accounted 491 for by the parameter R_{ai} from the CSDT. This approach also handled well the range of thicknesses 492 studied (Figure 14d). Although

the range of thickness studied is not representative of solid slab 493 bridges [10], the available results are of interest for slab-between-girders bridges. Moreover, the

494 studied approach enabled accurate predictions, regardless of the shear slenderness parameter *M/Vd* 495 (Figure 14f).

496 **5.4 Comparison with design code provisions**

497 Table 8 shows a comparison of different code-based approaches for the one-way shear capacity 498 of the experiments gathered in database B1 described in Section 3. The French model is used for 499 determining the effective width in combination with code provisions from Europe [50,56] and North 500 America [84]. The *fib* Model Code 2010 [34] is the only code which includes guidance for improved 501 arching action and effective width for concentrated loads close to the support. The same factor β_{prop} 502 for use with the CSDT was adopted in combination with the Swiss code SIA 262:2013 model [56]
503 and with the AASHTO code provisions for bridges [84].

504 Table 8 - Statistics of V_{exp}/V_{calc} according to the range of shear slenderness λ= *M/Vd* for different
505 design code approaches.

b_{eff}	French GES	$\frac{V_{exp,red}}{V_{exp,red}}$	French	$\frac{V_{exp,red}}{V_{red}}$	French	$\frac{V_{exp,}}{V_{exp,}}$	*fib* MC	$\frac{V_{exp,}}{V_{red}}$	$\beta_{arching}$	$\frac{V_{exp,}}{V_{CSDT}}$	Prop	$\frac{V_{exp,}}{V_{CSDT}}$	Prop	*AASHTO*	Prop	*CEN* 04	Prop	*MC*	*SIA* 262
AVG	1.044	1.043	1.421	1.704	1.762	1.096													
MIN	0.773	0.748	0.986	1.095	1.176	0.819													
<2.5	55																		
COV	11.4%	12.2%	16.5%	18.0%	22.6%	14.8%													
AVG	1.070	1.295	1.476	1.122	1.479	1.037													
MIN	0.723	0.830	0.918	0.606	0.749	0.733													
>2.5	86																		
COV	15.8%	19.2%	33.3%	24.0%	29.0%	16.4%													
AVG	1.060	1.197	1.454	1.349	1.589	1.060													
MIN	0.723	0.748	0.918	0.606	0.749	0.733													
All	141																		
COV	14.3%	20.3%	28.2%	29.8%	27.6%	15.9%													

507 Table 8 shows that the code provisions studied provided a mean ratio of V_{exp}/V_{cal} between 508 1.043 and 1.704 for λ < 2.5. The most precise results were achieved by the French effective shear 509 width model combined with the one-way shear model based on the CSDT, as proposed in this study 510 when the governing failure mode is known and is one-way shear. The predictions with the AASHTO 511 code provisions were more conservative, with a mean ratio between experimental and calculated 512 shear strengths higher than 1.4 on both ranges of shear slenderness studied.

513 Table 8 also shows that the average ratio of V_{exp}/V_{cal} ranged from 1.060 to 1.589 for a shear 514 slenderness higher than 2.5. Remarkably, the Swiss code provisions reached the same level of 515 accuracy and precision of CSDT when combined with the French model of effective shear width and 516 use of β_{prop}. Although these models (CSDT and SIA 262:2013) were derived in different ways, this 517 result occurs because both models rely on some similar ideas, such as the higher influence of 518 aggregate interlock in the shear strength and the decrease of the shear strength for increasing shear 519 slenderness. Since both AASHTO models and *fib* Model Code Models were derived based on the 520 Simplified Modified Compression Field Theory (SMCFT [78]), the statistical differences can be 521 attributed to the models to account for improved arching action and the effective shear width used.

522 **5.5 Test with double loads**

523 The number of tests with double loads parallel to line supports is very limited. There are only 524 8 tests in the literature conducted by Rombach and Henze [85], Vaz Rodrigues et al. [19] and Reiβen 525 et al. [3]. Most of these tests were conducted on cantilever slabs (7/8). The test with 4 loads close to 526 the line support conducted by Vaz Rodrigues [19] showed a punching failure and was not analyzed 527 in this study because it showed a transitional failure between the one-way and two-way shear. Table 528 9 shows the statics of the ratio between experimental and predicted one-way shear resistances for 529 these tests. In summary, the level of accuracy of the CSDT model combined with the French effective 530 shear width was close to that of slabs subjected to a single load. However, additional tests are needed 531 to confirm these findings. The most unsafe prediction in Table 9 (V_{exp}/V_{pred} = 0.89) occurred for the 532 only test with a ratio $a_v/d < 2.5$. Therefore, the proposed factor to consider arching action (β_{prop}) may 533 have been too optimistic for this type of loading.

534

535

536 Table 9 - Statistical of the experimental to calculated shear strengths for tests with double loads
537 close to a line support.

Authors	Test	$V_{exp,red}/V_{CSDT\ beff,French}$
Vaz Rodrigues et al [19]	DR1b	1.26
	DR2a	1.03
	DR2b	1.07
Rombach & Henze [85]	2*d* x 2	0.89
	3*d* x 2	0.99
	4*d* x 2	1.06
	5*d* x 2	1.01
Reiβen et al. [3]	MS35BB-22	1.04
	AVG	1.04
	COV (%)	9.78

538

539 **5.6 General approach for one-way and two-way shear**

540 An alternative approach to assessing the one-way shear models applicable to members with 541 possible punching failure is to decrease the effective shear width accordingly with the shear 542 slenderness, as discussed in the proposed GESW model (Section 4). In this study, we assumed that 543 the French effective shear width should be multiplied by the parameter α (Equation (42)).

544 Table 10 shows the statistics of the ratio between experimental and predicted shear capacities 545 with one-way and two-way shear models according to the failure mode for the database with 214 test 546 results of slabs under single concentrated loads (Database B0). For the punching shear provisions, the 547 proposed model from prEN 1992-1-1:2018 [86] was used (based on the CSCT), while for the one

548 way shear models we combined the CSDT models with the French and GESW models. Table 10 549

shows that the level of precision reached with the CSDT combined with the GESW model is very similar for both failure modes, while the other approaches provide precise estimations only for their respective failure modes.

Table 10 - Comparison of predictions with the CSDT for one-way shear and the punching shear provisions from prEN 1992-1-1:2018 [86] according to the failure mode.

Failure mode	Nº		$\frac{P_{exp}}{P_{EC18}}$	$\frac{V_{exp,red}}{V_{CSDT}}$	$\frac{V_{exp,red}}{V_{CSDT}}$
		b_{eff}	-	French	GESW
P	51	AVG	1.092	0.808	1.044
		MIN	0.724	0.331	0.712
		COV	20.0%	31.6%	21.2%
WB	141	AVG	1.219	1.060	1.197
		MIN	0.466	0.723	0.748
		COV	31.9%	14.3%	20.3%
WB/P	22	AVG	1.220	1.007	1.121
		MIN	0.942	0.712	0.833
		COV	21.5%	13.4%	15.6%
All	214	AVG	1.189	0.994	1.153
		MIN	0.466	0.331	0.712
		COV	29.2%	21.0%	20.8%

6 DISCUSSIONS

Previous publications on the field of one-way slabs under concentrated loads usually concentrate on the accuracy of semi-empirical models applied to reduced databases [10,11]. When mechanical-based models are investigated, usually the analyses concentrate on one kind of support condition [15]. Most of them neglect the governing failure mode of the tests [11,87]. Therefore, a gap of more comprehensive studies is realized related to the shear capacity of slabs under concentrated loads failing in different modes.

Tests with a presumed punching failure were initially removed from the database B1. Only members with predominant one-way shear failure were used in the firststatistical analyses. Therefore, part of the higher level of accuracy in Section 5.2 with the French effective shear width can be attributed to the improved database selection. However, we have highlighted that the classification of the failure modes for some members may not be an easy task. For such cases, the experiments must be classified as governed by a mixed failure between one-way shear and two-way shear, as made in previous publications [10]. In these tests, both conical cracks at the top/bottom face and flexure-shear cracks at the edges of the slab arise at failure. Some studies have claimed that one-way and two-way shear capacities can be very similar is terms of strength ratio (V_{exp}/V_{calc} similar to P_{exp}/P_{calc}) [20], which was also verified in this study for some tests during the classification of the failure modes. Particularly, this is also in line with the ACI 318-19 punching provisions [88], where the punching capacity is assumed to be governed by one-way shear when the load becomes very rectangular.

Since most mechanical models, such as the CSDT [6], CSCT [77], and SMCFT [78] were derived from flexure-shear failures, one could question their possible extension to non-slender members, whose predominant failure mode is a shear-compression failure. In fact, some studies, as well as the current ACI 318-19 [88], have highlighted those members should be assessed by strut and-tie models, instead of sectional strain-based models [89,90]. However, most engineers have raised the possibility of covering a more extensive range of cases with the same model. In particular, for the shear assessment of existing RC slab bridges, there is a need for uniform approaches that allow

582 checking all cross-sections and load positions in a preprogrammed way. Such an approach requires 583 the checking of modelsfor non-slender members in an approach similar to the one suggested in design 584 guides, e.g., NEN 1992-1-1:2005 [50] and *fib* Model Code 2010 [34], i.e. based on the reduction of 585 the acting shear load close to the support. We have highlighted that such analyses should be used only

586 as a first assessment of structures without stirrups. As such, they are in line with the need for a 587 preprogrammed method for the assessment of a large number of existing RC slab bridges.

588 The level of accuracy reached by the CSDT with our method for arching action and the French 589 model of effective width is similar to that obtained by the CSCT [2], but removes the need for finite 590 element calculations. The proposed CSDT extension excels due to its easy application. The overall 591 V_{exp}/V_{cal} average ratio with the CSDT is 1.06, with a 14.3% coefficient of variation for a set with 141

592 test results. Comparatively, Natário [2] achieved a 1.12 V_{exp}/V_{calc} average ratio with 11% COV for 593 simply supported members (62 tests) and 1.07 AVG and 16% COV for cantilever members (27 tests). 594 However, Natário's study did not include continuous members or members with combinations of 595 loads (concentrated loads combined with line loads). The database B0 has 33 tests with loads close 596 to continuous supports. The mean ratio between experimental and predicted shear capacities by the 597 CSDT model with the French effective shear width and β_{prop} is 1.01 with a COV of 11.3%. Therefore, 598 this study comprehends a larger variety of support and loading conditions. The narrow scatter between 599 experimental and predicted shear capacities with the CSDT demonstrates its accuracy and precision 600 in assessing the one-way shear capacity of wide RC members under concentrated loads, such as slab 601 bridges.

602 Different from other studies [15,28], we have identified that the use of the French approach 603 for determining the effective shear width provides reasonable levels of accuracy combined with the 604 one-way shear strength model based on the CSDT. Regarding studies on simply supported members 605 in which the French model leads to unsafe predictions of the shear strength [15,28], our analysis 606 indicates that these experiments presented signals of punching failures and, therefore, should also be 607 evaluated by two-way shear strength models to reach more precise predictions.

608 Notably, the CSDT combined with the GESW model provides homogeneous levels of 609 precision in predicting the shear capacity for specimens with one-way and two-way shear failures in 610 the database B0, capturing well the complex transition between these two failure modes. The reason 611 for this observation is that the precision and accuracy of the predictions with the GESW model were 612 similar between different failure modes, shear slenderness, and support conditions. In addition, the 613 level of precision was considerably better than that obtained with current semi-empirical code models 614 [10,87], for which COVs are usually larger than 35%. Therefore, in a programmed approach of 615 assessment, the CSDT combined with the GESW model may be used as the only model to check 616 shear failures when the governing failure mode is unknown.

7 CONCLUSIONS

This study presents an extension of the Critical Shear Displacement Theory model for wide members under concentrated loads. Different databases were used to assess (i) the proposed arching action factor, (ii) the accuracy and precision of the CSDT combined with different models of effective shear width for slabs under single concentrated loads; (iii) the accuracy of the CSDT model to assess members with double concentrated loads parallel to the support and (iv) to assess slabs that showed different failures modes in shear. The following can be concluded:

1. The model for improved arching action for non-slender members can be combined with the CSDT as a first step for the determination of their shear strength. This approach was validated against databases of wide members loaded over the entire width, as well as for slabs under concentrated loads failing in one-way shear.

2. The CSDT, combined with the effective width model from the French design guides [32], provides accurate results of shear strength for wide members with predominant one-way shear failure, regardless of the shear slenderness and support conditions. The same level of precision was reached for slabs under double concentrated loads parallel to the support.

3. The level of accuracy of our proposed approach based on the CSDT combined with the French effective shear width was higher than that of most design code models, regardless of the parameters analyzed. Since our approach requires only analytical calculations (without finite element analysis), it can easily be implemented in the daily engineering practice for first levels of approximation.

4. Despite the simplicity of the French effective width model, it seems to represent well most one-way shear tests investigated. However, for members with punching failure, the approach may lead to unsafe predictions of shear strength, as verified in this study. Since the governing failure mode may not be known in preliminary analyses, both failure modes must be checked in the daily engineering practice for higher levels of approximation.

5. The most general effective shear width model (GESW) leads to good levels of accuracy for slabs

under concentrated loads since it deals with both one-way and two-way shear failures. 644 Moreover, the proposed approach addresses in a novel manner the transition between one-way shear 645 and two-way shear failures of slabs under concentrated loads. However, it should be highlighted that 646 this approach should be used only for preliminary designs and global assessment of a large number 647 of assets, since it does not determine the governing failure mode physically. Apart from that, further 648 studies are required in order to include the effects of other parameters, such as the slab width b in the 649 transition between one-way and two-way shear failures.

650 6. This study shows that traditional models of effective shear width and punching shear do not 651 provide precise predictions of shear strength when the critical failure mode is other than that assumed 652 by the model (Section 5.6). Because of this, adjustments are required on each model to extend the 653 applications of them for both failure modes. In this study, different approaches are shown to assess 654 the shear capacity when the governing failure mode is known or unknown. The proposed approaches 655 apply to wide beams and slabs under different support conditions (simple, continuous, and cantilever 656 support), different loading conditions (loaded over the entire width or concentrated on the width 657 direction).

658 **DECLARATION OF CONFLIT INTEREST**

659 The authors declare that they have no known competing financial interest or personal 660 relationships that could have appeared to influence the work reported in this paper.

661 **CREDIT AUTHORSHIP CONTRIBUTION STATEMENT**

662 Alex de Sousa: Conceptualization, Methodology, Resources, Data curation, Writing - original 663 draft, preparation. Eva Lantsoght: Conceptualization, Supervision, Writing - review & editing. 664 Yuguang Yang: Supervision, Writing - review & editing. Mounir El Debs: Supervision, Project 665 administration, Funding acquisition & manuscript review.

666 **ACKNOWLEDGMENTS**

667 The authors acknowledge the financial support provided by the Brazilian National Council for 668 Scientific and Technological Development (CNPq) and the São Paulo Research Foundation (FAPESP 669

2018/21573-2 and FAPESP 2019/20092-3) and Angela Pregnolato Giampedro for the English 670 language revision.

671

672 **NOTATION**

Notation Description

a shear span: distance between the center of the support and the center of the load a_v clear shear span: distance between face of support and face of load *b* width of the structural member

b_n clear width of the structural member
d effective depth of longitudinal reinforcement
d_t effective depth of transverse reinforcement
d_g maximum aggregate size
f_c concrete compressive strength
f_{ck} characteristic concrete compressive strength
f_{cm} mean value of cylinder compressive strength of concrete
f_y yield strength of reinforcement
k_c slope of stress line, $k_c = 1.28$ according to [91]
m_{Ed} design (factored) moment per unit length in critical section
m_{Rd} plastic design (factored) moment per unit length in critical section n_e *or* n ratio between elastic modulus of steel and concrete
$l_{cr,m}$ spacing of two neighboring major cracks
$s_{cr,CSDT}$ height of fully developed crack
s_{rm} crack spacing of primary cracks
w crack width
w_b crack width at the bottom of the crack
x neutral axis depth
z length of internal level arm or effective shear depth according to *fib* MC 2010, taken as $0.9d$
A_x, A_y projected areas of a cracked surface for a unit crack length in two directions A_s longitudinal reinforcement area
A_g gross area of concrete section
E_c modulus of elasticity of concrete
E_s elastic modulus of steel
G_c modulus of shear deformation for un-cracked concrete chord
G_f concrete fracture energy
M cross-sectional bending moment
M_{Ed} design sectional moment
N_{Ed} design sectional axial load
P_{exp} measured peak load in an experiment
P_{EN18} Predicted punching capacity by prEN 1992-1-1:2018 [86]
V shear force
V_{ai} shear force transferred by aggregate interlock
V_c shear force transferred in concrete compression zone
V_d shear force transferred by dowel action
V_{Ed} design shear force
V_{exp} Experimental shear force strength from the database tests
$V_{exp,red}$ Experimental shear force reduced by the parameter β
V_{cal} Calculated shear force strength
V_{AASHTO} one-way shear capacity calculated according to AASHTO
V_{CEN} one-way shear capacity calculated according to NEN 1992-1-1:2005 V_{ACI-19} one-way shear capacity calculated according to ACI 318-19
V_{MC} one-way shear capacity calculated according to Model Code 2010

V_{SIA} one-way shear capacity calculated according to SIA 262:2013
V_{CSDT} one-way shear capacity calculated according to CSDT
α_e modular ratio (E_s/E_c)
β reduction factor for the contribution of loads close to the support to the shear force γ_c partial safety factor for concrete
Δ shear displacement at crack
Δ_{cr} critical shear displacement
Δ_e distance between neutral axis and center of internal lever arm z
ε_s steel strain

ε_x longitudinal strain at mid-depth of the effective shear depth
ϕ rebar diameter
$\mu_{,CSDT}$ friction coefficient for contact area between aggregate particles and matrix with μ = 0.4proposed according to Walraven [92]
ρ_s longitudinal reinforcement ratio
σ normal stress
σ_{pu} crushing (yielding) strength of matrix, or contact stress at cracked surface τ shear stress
τ_{ai} shear stress transferred by aggregate interlock
τ_{Rd} design shear capacity of concrete
τ_c concrete shear capacity
AVG Average value
COV coefficient of variation
CSCT Critical Shear Crack Theory
CSDT Critical Shear Displacement Theory
SMCFT Simplified Modified Compression Field Theory
MIN Minimum value

673

674 **REFERENCES**

675 [1] Lantsoght EOL, Van Der Veen C, Walraven JC. Shear in One-Way Slabs under 676 Concentrated Load Close to Support. ACI Struct J 2013;110.

677 [2] Natário F, Fernández Ruiz M, Muttoni A. Shear strength of RC slabs under concentrated 678 loads near clamped linear supports. Eng Struct 2014;76:10–23.
679 https://doi.org/10.1016/j.engstruct.2014.06.036.

680 [3] Reiβen K, Classen M, Hegger J. Shear in reinforced concrete slabs-Experimental 681 investigations in the effective shear width of one-way slabs under concentrated loads and 682 with

different degrees of rotational restraint. Struct Concr 2018;19:36–48. 683
https://doi.org/10.1002/suco.201700067.

684 [4] Henze L, Harter M, Rombach GA. Querkrafttragfähigkeit von Stahlbetonplatten ohne 685
Querkraftbewehrung unter konzentrierten Einzellasten (Shear capacity of reinforced concrete 686 slabs
without transverse reinforcement under concentrated loads Part 2: Proposal for a new 687 design model).
Beton- Und Stahlbetonbau 2019. https://doi.org/10.1002/best.201800106.

688 [5] de Sousa AMD, Lantsoght EOL, El Debs MK. One-way shear strength of wide reinforced 689
concrete members without stirrups. Struct Concr 2020:1–25.
690 https://doi.org/10.1002/suco.202000034.

691 [6] Yang Y, den Uijl J, Walraven J. Critical shear displacement theory: on the way to extending 692
the scope of shear design and assessment for members without shear reinforcement. Struct 693 Concr
2016;17:790–8. https://doi.org/10.1002/suco.201500135.

694 [7] Yang Y, Walraven J, Uijl J den. Shear Behavior of Reinforced Concrete Beams without 695
Transverse Reinforcement Based on Critical Shear Displacement. J Struct Eng 696
2017;143:04016146. https://doi.org/10.1061/(ASCE)ST.1943-541X.0001608.

697 [8] Gurutzeaga M, Oller E, Ribas C, Cladera A, Marí A. Influence of the longitudinal 698
reinforcement on the shear strength of one-way concrete slabs. Mater Struct Constr 699
2015;48:2597–612. https://doi.org/10.1617/s11527-014-0340-5.

700 [9] Conforti A, Minelli F, Plizzari GA. Influence of width-to-effective depth ratio on shear 701
strength of reinforced concrete elements without web reinforcement. ACI Struct J 702
2017;114:995–1006. https://doi.org/10.14359/51689681.

703 [10] Lantsoght EOL, van der Veen C, Walraven JC, de Boer A. Database of wide concrete 704
members failing in shear. Mag Concr Res 2015;67:33–52.
705 https://doi.org/10.1680/macr.14.00137.

706 [11] Henze L, Rombach GA, Harter M. New approach for shear design of reinforced concrete 707
slabs under concentrated loads based on tests and statistical analysis. Eng Struct 708
2020;219:110795. https://doi.org/10.1016/j.engstruct.2020.110795.

709 [12] Reiβen K, Hegger J. Experimentelle Untersuchungen zum Querkrafttragverhalten von 710
auskragenden Fahrbahnplatten unter Radlasten. Beton- Und Stahlbetonbau 2013;108:315–24. 711
https://doi.org/10.1002/best.201200072.

712 [13] Reißen K, Hegger J. Experimentelle Untersuchungen zur mitwirkenden Breite für Querkraft 713
von einfeldrigen Fahrbahnplatten. Beton- Und Stahlbetonbau 2013;108:96–103. 714
https://doi.org/10.1002/best.201200064.

715 [14] Lantsoght EOL, van der Veen C, Walraven J, de Boer A. Experimental investigation on shear 716
capacity of reinforced concrete slabs with plain bars and slabs on elastomeric bearings. Eng

717 Struct 2015;103:1–14. https://doi.org/10.1016/J.ENGSTRUCT.2015.08.028.

718 [15] Halvonik J, Vidaković A, Vida R. Shear Capacity of Clamped Deck Slabs Subjected to a 719
Concentrated Load. J Bridg Eng 2020;25:04020037.
720 https://doi.org/10.1061/(ASCE)BE.1943-5592.0001564.

721 [16] Bui TT, Abouri S, Limam A, NaNa WSA, Tedoldi B, Roure T. Experimental investigation of 722
shear strength of full-scale concrete slabs subjected to concentrated loads in nuclear 723 buildings. Eng
Struct 2017;131:405–20. https://doi.org/10.1016/j.engstruct.2016.10.045.

724 [17] Lantsoght EOL, van der Veen C, Walraven JC, de Boer A. Transition from one-way to two 725
way shear in slabs under concentrated loads. Mag Concr Res 2015;67:909–22. 726
https://doi.org/10.1680/macr.14.00124.

727 [18] Muttoni A, Fernandez Ruiz M. Shear in slabs and beams: should they be treated in the same 728 way? Fédération Int. du Bét. Bull. N°57, 2010, p. 105–28.

729 [19] Vaz Rodrigues R, Fernández Ruiz M, Muttoni A. Shear strength of R/C bridge cantilever 730 slabs. Eng Struct 2008;30:3024–33. https://doi.org/10.1016/j.engstruct.2008.04.017.

731 [20] Natário F. Static and Fatigue Shear Strength of Reinforced Concrete Slabs Under 732 Concentrated Loads Near Linear Support. Thesis (Docteur ès Sciences) - Faculté de 733 L'environnement Naturel, Architectural et Construit Laboratoire de Construction en Béton, 734 École Polytechnique Fédérale de Lausanne, 2015. https://doi.org/10.5075/epfl-thesis-6670.

735 [21] Reiβen K. Zum Querkrafttragverhalten von einachsig gespannten Stahlbe- tonplatten ohne 736 Querkraftbewehrung unter Einzellasten. PhD Thesis (Doctor of Engineering), Faculty of 737 Civil Engineering, RWTH Aachen University, 2016.

738 [22] Henze L. Querkrafttragverhalten von Stahlbeton-Fahrbahnplatten. PhD Thesis, Institute for 739 Concrete Structures, Technische Universität Hamburg (TUHH), 2019.

740 [23] Doorgeest J. Transition Between One-way Shear and Punching Shear. Master of Science 741 Thesis, Delft University of Technology, 2012.

742 [24] Regan PE. Shear Resistance of Members without Shear Reinforcement; Proposal for CEB 743 Model Code MC90 1987:1–28.

744 [25] Lantsoght EOL, Van Der Veen C, De Boer A, Walraven JC. Transverse load redistribution 745 and effective shear width in reinforced concrete slabs. Heron 2015;60:145–79.

746 [26] Lantsoght EOL, de Boer A, van der Veen C. Distribution of peak shear stress in finite 747 element models of reinforced concrete slabs. Eng Struct 2017;148:571–83. 748 https://doi.org/10.1016/j.engstruct.2017.07.005.

749 [27] Sagaseta J, Tassinari L, Fernández Ruiz M, Muttoni A. Punching of flat slabs supported on 750 rectangular columns. Eng Struct 2014;77:17–33.
751 https://doi.org/10.1016/j.engstruct.2014.07.007.

752 [28] Reiβen K, Hegger J. Experimental investigations on the effective width for shear. 753 Maintenance, Monit. Safety, Risk Resil. Bridg. Bridg. Networks - Proc. 8th Int. Conf. Bridg. 754 Maintenance, Saf. Manag. IABMAS 2016, 2016, p. 2340–8.

755 [29] Lantsoght EOL, de Boer A, van der Veen C, Walraven JC. Effective shear width of concrete 756 slab bridges. Proc Inst Civ Eng - Bridg Eng 2015;168:287–98.
757 https://doi.org/10.1680/bren.13.00027.

758 [30] ABNT NBR 6118. NBR 6118: Design and execution of reinforced concrete buildings (in 759 portuguese). Rio de Janeiro: Associação Brasileira de Normas Técnicas (ABNT); 1980.

760 [31] NORMCOMISSIE 351001. NEN 6720 Technische Grondslagen voor Bouwvoorschriften 761 1995.

762 [32] FD P 18-717. Eurocode 2 - Calcul des structures en béton - Guide d'application des normes 763 NF EN 1992 2013.

764 [33] Grasser E, Thielen G. Hilfsmittel zur Berechnung der Schnittgrößen und Formänderungen von Stahlbetontragwerken : nach DIN 1045, Ausg. Juli 1988. 3°
765 revised. Berlin: Beuth 766 Verlag GmbH; 1991.

767 [34] Fédération Internationale du Béton (fib). fib Model Code for Concrete Structures 2010. vol. 768 Vol. 1-2. Lausanne, Switzerland: Ernst & Sohn - fédération internationale du béton, Bulletin 769 65; 2012.

770 [35] Bauer T, Müller M. Straßenbrücken in Massivbauweise nach DIN- Fachbericht - Beispiele 771

prüffähiger Standsicherheitsnachweise. 2. Auflage. Berlin: Bauwerk; 2003.

772 [36] Vidakovi A, Halvonik J. Shear resistance of clamped deck slabs assessed using design 773 equations and FEM analysis. 13th Int. Conf. Mod. Build. Mater. Struct. Tech., 2019, p. 0–7.

774 [37] Johansen KW. Yield-Line Formulae for Slabs. CRC Press Yea; 2005.

775 [38] Goldbeck AT. The Influence of Total Width of the Effective Width of Reinforced-Concrete 776 Slabs Subjected to Cental Concentrated Loading. ACI J Proc 1917;13:78–88. 777 https://doi.org/10.14359/15865.

778 [39] DAfStb. Deutscher Ausschuss für Stahlbeton Heft 240: Hilfsmittel zur Berechnung der 779 Schnittgrößen und Formänderungen von Stahlbetonbauwerken. (German Committee for 780 Structural Concrete Book 240: Tools for calculation of internal forces and changes in shape 781 of rein. Berlin / Germany: Beuth Verlag; 1991.

782 [40] BBK (Statens Betong Kommitte). Regulations for concrete structures – Part 1: Design. BBK, 783 Stockholm, Sweden; 1979.

784 [41] Zheng Y, Taylor S, Robinson D, Cleland D. Investigation of ultimate strength of deck slabs 785 in steel-concrete bridges. ACI Struct J 2010;107:82–91.

786 [42] Reiβen K, Hegger J. Shear Capacity of Reinforced Concrete Slabs under Concentrated 787 Loads. 8th IABSE Congr. 2012 "Innovative Infrastructures - Towar. Hum. Urban., Seoul, 788 Südkorea,: 2012. https://doi.org/10.2749/222137912805111320.

789 [43] Reiβen K, Hegger J. Numerical investigations on the shear capacity of reinforced concrete 790 slabs under concentrated loads. Res. Appl. Struct. Eng. Mech. Comput., CRC Press; 2013, p. 791 1507–12. https://doi.org/10.1201/b15963-271.

792 [44] Rombach GA, Velasco RR. Schnittgrößen auskragender fahrbahnplatten infolge von 793 radlasten nach DIN-fachbericht. Beton- Und Stahlbetonbau 2005;100:376–84. 794 https://doi.org/10.1002/best.200590093.

795 [45] Shu J, Plos M, Zandi K, Ashraf A. Distribution of shear force: A multi-level assessment of a 796 cantilever RC slab. Eng Struct 2019;190:345–59.
797 https://doi.org/10.1016/J.ENGSTRUCT.2019.04.045.

798 [46] Kani GNJ. The Riddle of Shear Failure and its Solution. ACI J Proc 1964;61:441–68. 799 https://doi.org/10.14359/7791.

800 [47] Leonhardt F, Walther R. Schubversuche an einfeldrigen Stahlbetonbalken mit und ohne 801 Schubbewehrung [Shear tests on single-span reinforced concrete beams with and without 802 shear reinforcement]. Berlin: Beuth; 1962.

803 [48] Cavagnis F, Fernández Ruiz M, Muttoni A. An analysis of the shear-transfer actions in 804 reinforced concrete members without transverse reinforcement based on refined experimental 805 measurements. Struct Concr 2018;19:49–64. https://doi.org/10.1002/suco.201700145.

806 [49] Bairán JM, Menduiña R, Marí A, Cladera A. Shear Strength of Non-Slender Reinforced 807 Concrete Beams. ACI Struct J 2020:277–90. https://doi.org/10.14359/51721369.

808 [50] CEN. EN 1992-1-1: Eurocode 2: Design of concrete structures -Part 1-1: General rules and 809 rules for buildings, EN 1992-1-1:2005 2005.

810 [51] Fernández Ruiz M, Muttoni A, Sagaseta J. Shear strength of concrete members without 811 transverse reinforcement: A mechanical approach to consistently account for size and strain 812 effects. Eng Struct 2015;99:360–72. https://doi.org/10.1016/J.ENGSTRUCT.2015.05.007.

813 [52] Kim D, Kim W, White RN. Arch Action in Reinforced Concrete Beams—A Rational 814 Prediction of Shear Strength. ACI Struct J 1999;96:586–93. https://doi.org/10.14359/695.

815 [53] ABNT NBR 6118. NBR 6118: Design of concrete structures — Procedure (in portuguese). 816 Rio de Janeiro: Associação Brasileira de Normas Técnicas (ABNT); 2014.

817 [54] DIN 1045. Beton und Stahlbeton - Bemessung und Ausführung. Berlin: Deutsches Institut 818 für Normung (DIN); 1988.

819 [55] DIN 1045-1. Bemessung und Konstruktion von Stahlbeton- und Spannbetonbauteilen. 820 Berlin: Deutsches Institut für Normung (DIN); 2001.

821 [56] SIA. Code 262 for concrete structures. Zürich: Swiss Society of Engineers and Architects; 822 2013.

823 [57] Yang Y, Uijl JA den, Walraven JC. Residual Shear Capacity of 50 years Old RC Solid Slab 824 Bridge Decks. Int. IABSE Conf. Assessment, Upgrad. Refurb. Infrastructures., Rotterdam: 825 2013, p. 538–9.

826 [58] Mörsch E. Der Eisenbetonbau [Concrete-steel construction]. New York.: Engineering News 827 Publishing; 1909.

828 [59] Baumann T, Rusch H. Versuche zum studien der verdübe- lungswirkung der 829 biegezugbewehrung eines stahlbetonbalkens [Exper- imental study on dowel action in 830 reinforced concrete beam]. Deutscher Ausschuss für Stahlbeton (DAfStb), Ernst, Berlin (in 831 German); 1970.

832 [60] Walraven JC. Fundamental Analysis of Aggregate Interlock. J Struct Div ASCE 833 1981;107:2245–2270.

834 [61] Chana PS. Investigation of the mechanism of shear failure of reinforced concrete beams. 835 Mag Concr Res 1987;39:196–204. https://doi.org/10.1680/macr.1987.39.141.196.

836 [62] Sousa AMD, Lantsoght EOL, El Debs MK. Database of wide beams and slabs under 837 concentrated loads failing in different shear failure modes. Zenodo 2020. 838 https://doi.org/10.5281/zenodo.4059803.

839 [63] Lantsoght EOL. Shear in Reinforced Concrete Slabs under Concentrated Loads Close to 840 Supports. Ph.D. Thesis , Faculty of Civil Engineering and Geosciences, Delft University of 841 Technology, 2013.

842 [64] Cullington DW, Daly AF, Hill ME. Assessment of reinforced concrete bridges: Collapse 843 tests on Thurloxton underpass. Bridg Manag 1996;Vol. 3:667–74.

844 [65] Lubell AS. Shear in Wide Reinforced Concrete Members. PhD dissertation. University of

845 Toronto, Canadá, 2006.

846 [66] Bui TT, Limam A, Nana W-S-A, Ferrier E, Bost M, Bui Q-B. Evaluation of one-way shear 847 behaviour of reinforced concrete slabs: experimental and numerical analysis. Eur J Environ 848 Civ Eng 2017:1–27. https://doi.org/10.1080/19648189.2017.1371646.

849 [67] Regan PE. Shear Resistance of Concrete Slabs at Concentrated Loads Close to Supports. 850 Polytechnic of Central London, UK, 1982.

851 [68] Regan PE, Rezai-Jorabi H. Shear Resistance of One-Way Slabs Under Concentrated Loads. 852 ACI Struct J 1988;85:150–7. https://doi.org/10.14359/2704.

853 [69] Vaz Rodrigues R, Muttoni A, Burdet O. Large Scale Tests on Bridge Slabs Cantilevers 854 Subjected to Traffic Loads. Proc. 2nd Int. Congr. fib, Naples, Italy: 2006.

855 [70] Rombach GA, Latte S. Shear resistance of bridge decks without shear reinforcement. Proc. 856 Int. fib Symp., Tailor Made Concrete Structures; 2008, p. 519–25. 857 https://doi.org/doi:10.1201/9781439828410.ch86.

858 [71] Rombach G, Latte S. Querkrafttragfähigkeit Von Fahrbahnplatten Ohne 859 Querkraftbewehrung. Beton- Und Stahlbetonbau 2009;104:642–56. 860 https://doi.org/10.1002/best.200900029.

861 [72] Natário F, Fernández Ruiz M, Muttoni A. Experimental investigation on fatigue of concrete 862 cantilever bridge deck slabs subjected to concentrated loads. Eng Struct 2015;89:191–203. 863 https://doi.org/10.1016/J.ENGSTRUCT.2015.02.010.

864 [73] Henze L, Rombach GA. Versuche zur Querkrafttragfähigkeit von Stahlbetonplatten unter 865 auflagernahen Einzellasten; Versuchsbericht (Experimental investigations on shear capacity 866 of concrete slabs with concentrated loads close to the support). Hamburg: 2017. 867 https://doi.org/10.15480/882.1443.

868 [74] Vida R, Halvonik J. Experimentálne overovanie šmykovej odolnosti mostovkových dosiek 869 (Experimental verification of shear resistance of bridge deck slabs). Inžinierske 870 Stavby/Inženýrské Stavby 2018:2–6.

871 [75] Reineck K-H, Bentz EC, Fitik B, Kuchma DA, Bayrak O. ACI-DAfStb Database of Shear 872 Tests on Slender Reinforced Concrete Beams without Stirrups. ACI Struct J 2013;110:867– 873 76. https://doi.org/10.14359/51685839.

874 [76] Collins MP, Bentz EC, Sherwood EG. Where is shear reinforcement required? Review of 875 research results and design procedures. ACI Struct J 2008;105:590–600. 876 https://doi.org/10.14359/19942.

877 [77] Muttoni A, Ruiz MF. Shear Strength of Members without Transverse Reinforcement as 878 Function of Critical Shear Crack Width. ACI Struct J 2008;105:163–72. 879 https://doi.org/10.14359/19731.

880 [78] Bentz EC, Vecchio FJ, Collins MP. Simplified modified compression field theory for 881 calculating shear strength of reinforced concrete elements. ACI Struct J 2006;103:614–24. 882 https://doi.org/10.14359/16438.

883 [79] Cavagnis F, Fernández Ruiz M, Muttoni A. Shear failures in reinforced concrete members 884 without transverse reinforcement: An analysis of the critical shear crack development on the 885 basis of test results. Eng Struct 2015;103:157–73.
886 https://doi.org/10.1016/j.engstruct.2015.09.015.

887 [80] Yang Y. Shear Behaviour of Reinforced Concrete Members without Shear Reinforcement: A

888 New Look at an Old Problem. Delft University of Technology, 2014.

889 [81] Mihaylov BI, Bentz EC, Collins MP. Two-parameter kinematic theory for shear behavior of 890 deep beams. ACI Struct J 2013;110:447–55. https://doi.org/10.14359/51685602.

891 [82] Lantsoght E, de Boer A, van der Veen C. Levels of approximation for the shear assessment 892 of reinforced concrete slab bridges. Struct Concr 2017;18:143–52. 893 https://doi.org/10.1002/suco.201600012.

894 [83] Bauer T, Müller M, Blase T. Strassenbrücken in Massivbauweise nach DIN-Fachbericht : 895 Beispiele prüffähiger Standsicherheitsnachweise ; Stahlbeton- und Spannbetonüberbau nach 896 DIN-Fachbericht 101 und 102 ; mit CD-ROM. Bauwerk; 2005.

897 [84] AASHTO. AASHTO LRFD Bridge Design Specifications. 8th Editio. Washington D.C.: 898 American Association of State Highway and Transportation Officials (AASHTO); 2017.

899 [85] Rombach G, Henze L. Querkrafttragfähigkeit von Stahlbetonplatten ohne 900 Querkraftbewehrung unter konzentrierten Einzellasten. Beton- Und Stahlbetonbau 901 2017;112:568–78. https://doi.org/10.1002/best.201700040.

902 [86] Muttoni A, Caldentey AP, Hegger J, Vill M, Shave JD, Menegotto M. PT-SC2-T1 D3BG - 903 Background documents to prEN 1992-1-1:2018 2018.

904 [87] Reiβen K, Hegger J. Database of shear tests on RC slabs without shear reinforcement under 905 concentrated loads – Assessment of design rules according to Eurocode 2. 16th Eur. Bridg. 906 Conf., Edinburgh, Scotland: 2015.

907 [88] ACI Committee 318. Building Code Requirements for Structural Concrete (ACI 318-19) 908 2019:988.

909 [89] Vollum RL, Fang L. Shear enhancement near supports in RC beams. Mag Concr Res 910 2015;67:443–58. https://doi.org/10.1680/macr.14.00309.

911 [90] Sagaseta J, Vollum RL. Shear design of short-span beams. Mag Concr Res 2010;62:267–82. 912 https://doi.org/10.1680/macr.2010.62.4.267.

913 [91] Krips M. Rißbreitenbeschränkung im Stahlbeton und Spannbeton (Crack width restriction in 914 reinforced concrete and prestressed concrete). Berlin: Ernst & Sohn; 1985.

915 [92] Walraven JC. Aggregate Interlock: a Theoretical and Experimental Analysis. PhD. Thesis, 916 Delft University of Technology, 1980.

917